Journal of Molecular Liquids 381 (2023) 121790

Contents lists available at ScienceDirect

Journal of Molecular Liquids

journal homepage: www.elsevier.com/locate/molliq

Linear relationship between emission quantum yield and Stokes shift in 3-styryl aza-coumarin based dyes in the presence of cyclodextrins

Jackson J. Alcázar [a,b], Luis García-Río [c], Agustín I. Robles [a], Luis Dinamarca-Villarroel [a], Angélica Fierro [a], José G. Santos [a,*], Margarita E. Aliaga [a,*]

[a] Facultad de Química y de Farmacia, Escuela de Química, Pontificia Universidad Católica de Chile, Casilla 306, Santiago 6094411, Chile
[b] Centro de Química Médica, Facultad de Medicina Clínica Alemana, Universidad del Desarrollo, Santiago 7780272, Chile
[c] Departamento de Química Física. Facultad de Química. Universidad de Santiago, 15782 Santiago, Spain

ARTICLE INFO

Article history:
Received 18 December 2022
Revised 11 March 2023
Accepted 1 April 2023
Available online 5 April 2023

Keywords:
Aza-Coumarin dyes
Intramolecular rotation
Intramolecular charge transfer
Cyclodextrin inclusion
Emission quantum yield
Stokes shift
Supramolecular chemistry

ABSTRACT

The effect of the cyclodextrins inclusion on the Stokes shifts and emission quantum yield of three 3-styryl aza-coumarin dyes (SACs) was experimentally and theoretically studied. Preliminary results show a relationship between the emission quantum yield and the calculated binding constants. Supramolecular inclusion was supported by changes in the fluorescence spectra, high-resolution mass spectrometry and molecular dynamics studies. 2,6-di-O-methyl-β-cyclodextrin (DM-β-CD) presented higher binding constants than β-cyclodextrin (β-CD), along with up to a 6-fold increase in emission quantum yield for the SACs. Additionally, a linear negative correlation was obtained between the Stokes shift and the emission quantum yield. This linear and empirical relationship was explained by the action of a unique intramolecular rotation and charge transfer phenomenon in the dyes, which was modulated by cyclodextrins, and supported by calculations based on density functional theory.

1. Introduction

The understanding of photophysical properties of fluorescent dyes, such as the Stokes shift and the quantum yield, is key in the design of new molecules with enhanced properties for specific applications in optical microscopy, sensing, photodynamic therapy, among others [1–3]. Generally, fluorescent dyes with large Stokes shifts contain a coumarin fragment as a fluorophore and their fluorescence quantum yields are relatively low in polar solvents [4]. The same occurs with dyes containing 4-aza-coumarin (analogous to coumarin). Nevertheless, substituting a C–H group for a nitrogen atom enables the observation of absorptions and emissions at longer wavelengths, which is ideal for imaging biological samples [5]. For this reason, aza-coumarins have been recently used in the detection of various analytes in biological systems [6–10].

In most cases, aza-coumarins have been designed by incorporating a styryl moiety as a binding and recognition unit in position 3 and a dialkylamino group in position 7 of the azacoumarin scaffold. These 3-styryl derivatives 7-(dialkylamino)-aza-coumarin (SACs) have presented interesting solvatochromic effects in relation to the nature of the solvent in which they have been dissolved [11]. SACs dissolved in polar solvents present large Stokes shifts which have been attributed to the stabilization of an excited state with a higher dipole moment than the ground state. The higher dipole moment of the excited state is a consequence of intramolecular charge transfer (ICT) or twisted intramolecular charge transfer (TICT) phenomena [12].

Both ICT and TICT mechanisms are responsible for Stokes shifts when the excited state lives long enough to be stabilized by the solvent or medium that surrounds it. Furthermore, these mechanisms are also responsible for the emission quantum yield. In SACs, ICT originates through a "push–pull" mechanism between the dialkylamino group as electron donor and the aza-lactone moiety as electron acceptor (especially heterocyclic nitrogen) [11,13]. When this mechanism does not take place in aza-coumarins or coumarins[14], the compounds are mostly nonfluorescent. In addition, the formation of a non-emissive TICT state in polar solvents has been associated with decreased fluorescence quantum yields [15–17]. This implies that emission increases in SACs could take place in environments where ICT is favored and / or the formation of a non-emissive TICT state is restricted. Although there is no theoretical relationship between the Stokes shift (SS) and the emission quantum yield (Φ_E), in SACs these parameters present a non-random behavior adjusting to a cubic polynomial curve in organic

* Corresponding authors.
E-mail addresses: jgsantos@uc.cl (J.G. Santos), mealiaga@uc.cl (M.E. Aliaga).

https://doi.org/10.1016/j.molliq.2023.121790
0167-7322/

solvents [11]. This has suggested that the effect of the solvent on the excited state (ICT state and / or TICT state) is affecting the SS and Φ_E in intrinsic proportions according to the nature of the solvent.

The relationship between SS and Φ_E could be consequence of the styryl group present in SACs. The styryl group confers two simple bonds to aza-coumarins that could rotate in the excited state forming a TICT state, causing a breakdown of the π-conjugation and an increase in the dipole moment. The same could happen to the single bond that binds the dialkylamino electron donating group. Thus, supramolecular confinement (host–guest) could affect these rotations and charge transfer along the structure of the SACs, affecting both SS and Φ_E and empirically relating them to each other. In this context, this work aims to study **SAC1-3** spectroscopically in the absence and presence of macrocycles β-cyclodextrin (β-CD) and 2,6-di-O-methyl-β-CD (DM-β-CD) (Fig. 1), which have the particularity of granting a confined and hydrophobic environment with different bonding abilities [18,37].

2. Experimental section

2.1. Materials and equipment

The fluorescein and solvents were purchased from Sigma-Aldrich. The β-CD and DM-β-CD macrocycles were supplied by Cyclolab R&D. All organic solvents and reagents were used as received. The compound 3-styryl derivatives of 7-(dialkylamino)-aza-coumarins (**SAC1-3**) were synthesized as previously described [13]. The absorption spectra were recorded on a Varian Cary 50 Scan UV Visible Spectrophotometer and the fluorescence spectra were taken using a Cary Eclipse fluorescence spectrometer. HR-MS experiments were carried out using a compact QqTOF instrument (Bruker).

2.2. Determination of binding constants of SAC1-3 in presence of cyclodextrins

The Binding constant values were determined by the non-linear regression method to fit the emission intensity at a fixed wavelength in the prepared solutions. The experimental data obtained were adjusted to the binding model of 1:1 stoichiometry (Scheme 1), making use of Eq. (1) [19].

$$I = \frac{(\varepsilon_{HG} - \varepsilon_G)}{2}\left(-b - \sqrt{b^2 - 4[H]_0[G]_0}\right) + \varepsilon_G[G]_0;\ with$$
$$b = -\left([H]_0 + [G]_0 + \frac{1}{K_{1:1}}\right) \quad (1)$$

$$H + G \rightleftharpoons^{K_{1:1}} HG$$

Scheme 1. Host–guest binding mechanism for a 1:1 stoichiometric ratio.

where $[H]_0$ and $[G]_0$ are the initial molar concentrations of the host and guest, and ε_G and ε_{HG} the constants of proportionality of the guest and complex at the measurement wavelength, respectively.

2.3. Determination of change in Stokes shift (ΔSS)

For each of the above solutions their emission spectra were evaluated using their respective absorption maximum wavelengths as excitation wavelengths. The maximum emission wavelength of both the substrate, λ_G^E, and the inclusion complex, λ_{GH}^E, expressed in nanometers, were used in the following equations:

$$SS_G(cm^{-1}) = 10^7\left(1/\lambda_G^A - 1/\lambda_G^E\right) \quad (2)$$

$$SS_{HG}(cm^{-1}) = 10^7\left(1/\lambda_{HG}^A - 1/\lambda_{HG}^E\right) \quad (3)$$

were SS_G and SS_{HG} are the Stokes shifts at cm^{-1}. The effect of the macrocycles on the Stokes shifts of the SACs (ΔSS) was obtained from the difference between SS_{HG} and SS_G:

$$\Delta SS = SS_{HG} - SS_G \quad (4)$$

2.4. Emission quantum yield (Φ_E)

A series of solutions was prepared in fluorometric cells with a 10-mm optical path. Each of the cells was prepared with different concentrations of substrate (**SAC1-3**) in methanol/water (3:7 v/v) with absorptions between 0 and 0.1 absorbance units at 25.0 °C. Emission spectra were then measured using the length of the absorption maximum as the excitation wavelength. Subsequently, for each emission spectrum obtained, the area under the curve was integrated to obtain the integrated emission intensity.

The same procedure was performed for **SAC1-3** in the presence of 1.5 mM β-CD and then 4.5 mM DM-β-CD, and for the fluorescein in 0.1 M of sodium hydroxide used as standard compound (η_R = 1.333, Φ_R = 0.925) [20].

Finally, the quantum yield of the samples (Φ_E) were determined using the Demas and Crosby equation (Eq. (5)) [21]:

$$\Phi_E = \Phi_R\left(\frac{S_x}{S_R}\right)\left(\frac{\eta_x^2}{\eta_R^2}\right) \quad (5)$$

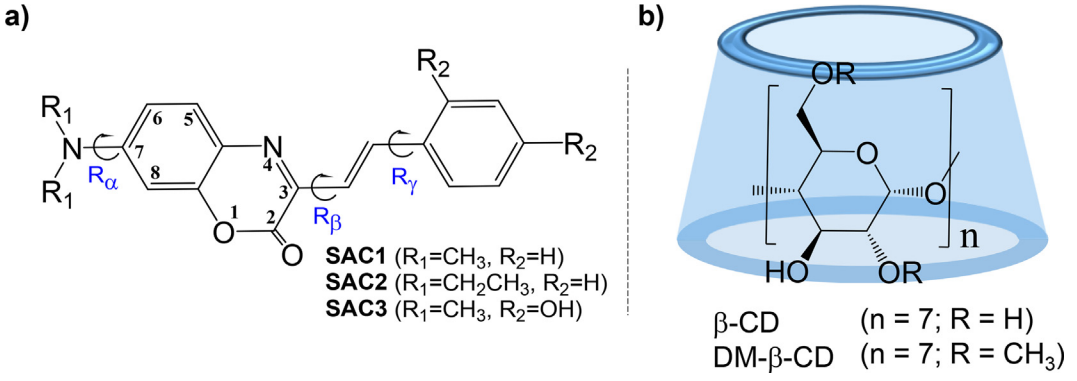

Fig. 1. Representation of: a) Homologues of 3-styryl derivatives of 7-(dialkylamino)-aza-coumarins (**SAC1-3**) with their respective rotations about single bonds (R_α, R_β and R_γ), b) β-cyclodextrin (β-CD) y 2,6-di-O-methyl-β-CD (DM-β-CD).

where Φ_E is the quantum yield, S is the gradient of the line (integrated emission intensity *versus* absorbance), η the refractive index of the solvent (3:7 v/v Methanol/water, η_x = 1.338) [22] and the subscripts R and × denote standard compound and sample, respectively.

It is important to mention that for complexes with β-CD, the Φ_E was obtained excluding the contribution of the free substrate in integrated emission intensity (see Supplementary material).

2.5. Computational methods

2.5.1. Molecular modeling calculations

SAC1-3 compounds were built using Spartan18 software while β-CD was obtained from protein data bank (PDBid 1BFN) [23]. The DM-β-CD was obtained from methylation of 1BFN. Geometrical optimization, charges calculation, docking studies and molecular dynamic simulations were carried out as previously described by us [13]. Each complex of β-CD@SACs and DM-β-CD@SACs was simulated during 200 ns in an isothermic-isobaric system.

2.5.2. DFT calculations

The optimization of the electronic structure, and the absorption and fluorescence properties of **SAC1-3** were performed at the B97-3c theoretical level [24,25]. For optimization routine, the default parameters for convergence under the protocol TightSCF were used. The calculations of excited-state were run using Time-Dependent Density Functional Theory (TDDFT). The exploration of the potential energy surface over the single-bond rotations (R_β and R_γ) was performed by relaxed surface scanning. The simulate the aqueous environment, water was included by implicit solvation under the Conductor-like Polarizable Continuum Model with COSMO epsilon function (CPCMC). All calculations were carried out using the ORCA program package (Program Version 5.0.3) [26].

3. Results and discussion

3.1. Dynamic simulations studies for 3-styryl aza-coumarin based dyes into β-CD and DM-β-CD.

Prior to experimentally investigating the interactions between 3-styryl aza-coumarin based dyes (**SAC1-3**) and macrocycles β-CD and DM-β-CD, molecular dynamic simulations where run in aqueous solution using explicit solvent models. The substrates were simulated in their neutral forms due to the low p*K*a value of the dialkylamino group, for example for the substrate **SAC1** its p*K*a value is 1.3 [13]. These simulations offer an approximation of the structure of the host–guest complex based on the stability of the dynamic system. Final conformations of SACs@β-CD complexes after 200 ns of molecular dynamics are shown in Fig. 2A-C.

Each complex SACs@β-CD remains stable during the simulation, with root-mean-square deviation (RMSD) values close to 2 Å (Fig. 3 A-C). **SAC1** and **SAC2** show a stable complex, stabilized by a hydrogen bond (HB) during the simulation. The stabilization by a HB in the portal of β-CD retains the heterocycle immersed in the cavity. A comparative ΔG analysis in Fig. 3G and 3H indicates a more stable system when diethylamino substituent is present (Fig. 4 A-C).

On the other hand, is possible to observe a higher exposure of the styryl group of **SAC3** (Fig. 2C) to the solvent which could be mediated by a hydrogen bond network favored by hydroxyl groups on the aromatic center (Fig. 3F) and consequently, the aza-coumarin ring is even more exposed to the solvent (Fig. 2C) in comparison to **SAC1** and **SAC2**. MM/PBSA calculations indicates a stable system with ΔG = −12.92 kcal/mol for **SAC3**.

In order to evaluate the effect of alkylation on CD and the stability of SACs@DM-β-CD complexes, we carried out molecular modeling studies using the same conditions as for SACs@β-CD.

Interestingly, molecular dynamic results show that at 200 ns complexes formed between SACs and DM-β-CD are more stable than those formed between the dyes and β-CD, RMSD < 1 Å (Fig. 3-A-C and 5A-C).

In fact, the final structural conformation of DM-β-CD during the simulation has an impact on the stability of the complexes. The higher compactness generated by the macrocycle in contact with SACs keeps the aza-coumarin moiety inside the cavity. The same was observed in β-CD. Each SACs@DM-β-CD complex generates hydrogen bonds during the simulation, being the SAC3@DM-β-CD complex the one that generates the most hydrogen bonds. In addition, the HB in SAC3@DM-β-CD were observed at shorter distances than in SAC3@β-CD, which could be associated to stronger interactions.

At this point, our results establish a favorable and permanent interaction of SACs with β-CD and DM-β-CD, but the latter shows better results energetically. Thus, the comparison of free energy distributions shows more negative binding free energy in SACs complexed with the DM-β-CD which would make it a better overall host compared to β-CD.

The energetic difference recorded in the different macrocycles (*i.e.* lower negative values of the free energy for β-CD) can be attributed to the fact that β-CD generates intramolecular hydrogen bonds which are at the expense of generating interactions with SACs derivatives. This is supported by the results shown in the Figs. 3 and 5, where the RMSD increases, and the free energy distributions are less favourable in β-CD than DM-β-CD.

3.2. Fluorescence behavior of 3-styryl aza-coumarin based dyes into β-CD and DM-β-CD and their associated binding constant.

The fluorescence spectra of **SAC1-3** at different concentrations of β-CD and DM-β-CD are shown in Fig. 6. The intensity and shift of the fluorescence bands increases as the concentration of the macrocycle increases. This may be due to the decrease in non-radiative pathways, consequence of the rotational restriction of the SACs in the complex. Also, the relocation of the guest in a more hydrophobic microenvironment could also contribute to the spectral changes observed in Fig. 6, in according with previous studies reported with organic solvents [11], where the intensity of SAC1 substrate emission tends to be higher when the polarity of the medium decreases in ensemble with short emission wavelengths.

On the other hand, information about the complex stoichiometry is derived from HR-MS experiments, which have demonstrated that SAC compounds form 1:1 adducts with β-CD, a representative example is presented in Fig. S2. Thus, the binding constants ($K_{1:1}$) were estimated from the fluorescence titrations data (Fig. S1), by using Eq. (1) and are shown in Table 1.

The good fit of the experimental data to Eq. (1) supports the formation of 1:1 complexes between **SAC1-3** dyes and β-CD and DM-β-CD macrocycles. Unfortunately, the non-observation of changes in the absorption spectra and the poor solubility of the substrates in water did not allow for the corroboration of these estimates by other techniques such as UV–vis spectrometry or nuclear magnetic resonance (NMR). However, the magnitudes of the $K_{1:1}$ obtained were consistent with those reported in the literature for aromatic guest-cyclodextrin inclusion complexes [27–30].

The estimated $K_{1:1}$ for the **SAC1-3** in presence of β-CD are similar (≈700 M^{-1}), with **SAC3** being the substrate with the lowest affinity (see Table 1). These results agree with the literature for inclusion complexes of benzene [27], phenols [28] and chrysin derivatives [29] for a 1:1 inclusion complex, where the β-CD/chrysin complex is disfavored when the phenyl group is substi-

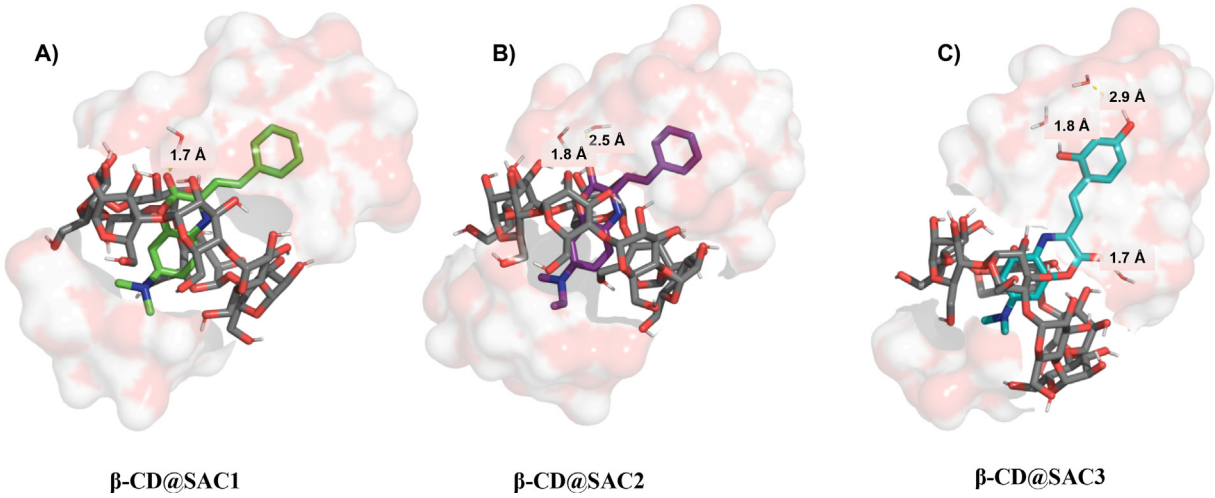

Fig. 2. Final conformations after 200 ns of molecular dynamic simulations of the β-CD complexes with the dyes (A) **SAC1** (green), (B) **SAC2** (purple) and (C) **SAC3** (cyan). Hydrogen bonds and their corresponding distances at 200 ns are displayed. (For interpretation of the references to colour in this figure legend, the reader is referred to the web version of this article.)

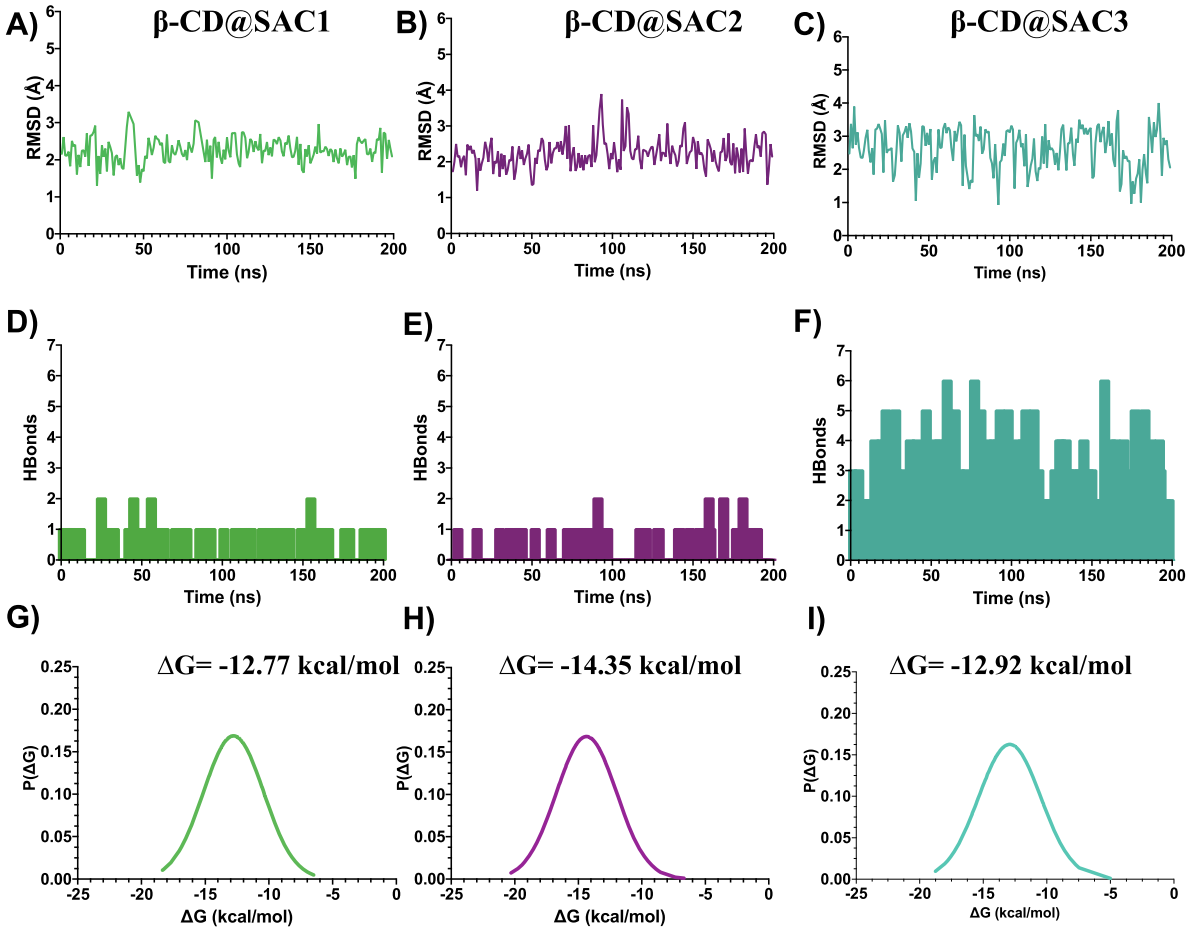

Fig. 3. Results from the molecular dynamic simulation of complexes SACs@β-CD during 200 ns. A-C) RMSD values shows stability of each complex during the simulation. D-F) Histograms of the number of HB present during the simulation. G-I) Free energy distribution from MM/PBSA calculations. Representations in green, purple and cyan are associated to **SAC1**, **SAC2** and **SAC3**, respectively. (For interpretation of the references to colour in this figure legend, the reader is referred to the web version of this article.)

tuted by a hydroxyl group [29]. In the presence of DM-β-CD, the complexes SAC1@DM-β-CD and SAC2@DM-β-CD presented similar $K_{1:1}$ (≈8900 M^{-1}), while the complex SAC3@DM-β-CD presented a $K_{1:1}$ 2.4 times higher. This suggests that: a) the alkyl chain of the dialkylamino group of SACs does not contribute to host–guest interaction, which is reasonable since the -NR_2 group of SACs is a very weak base (pK_a ≈ 1.5) [13] and b) the SAC3@DM-β-CD complex is favored by hydrogen bond formation between the hydroxyl

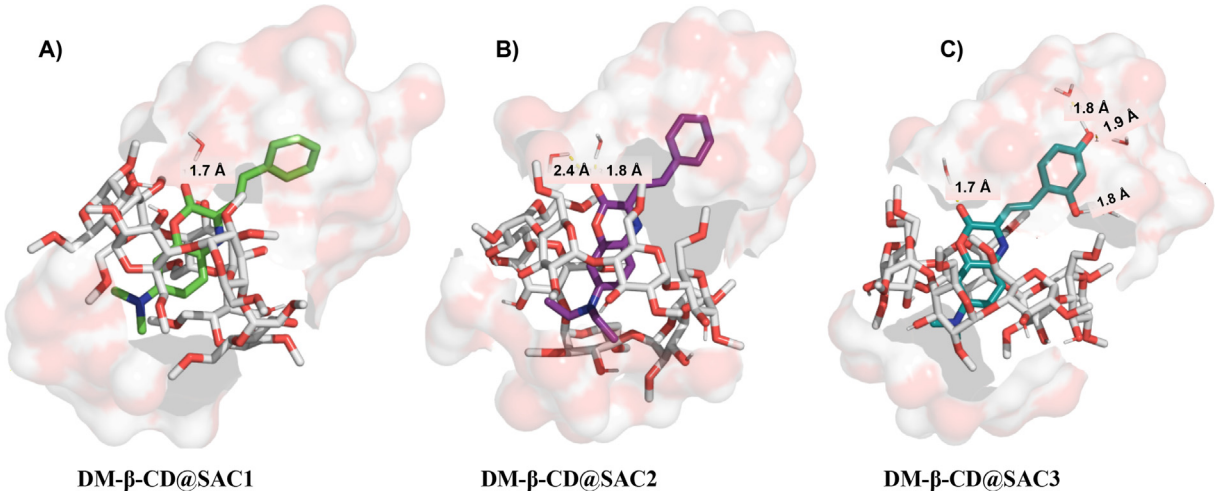

Fig. 4. Final conformations from molecular dynamic simulations of the DM-β-CD complexes with the dyes **(A) SAC1, (B) SAC2** and **(C) SAC3.**

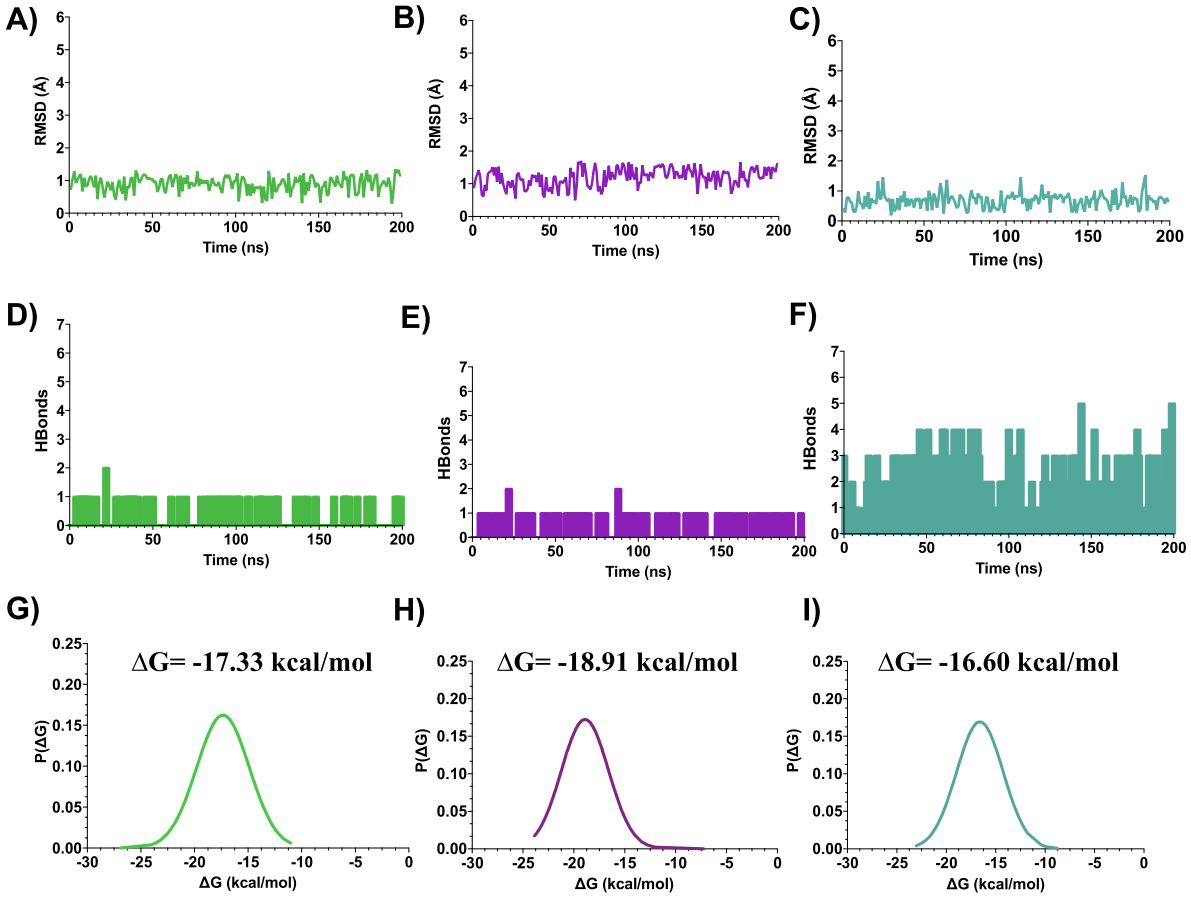

Fig. 5. Results from molecular dynamic simulation of complexes SACs@DM-β-CD during 200 ns. A-C) RMSD values shows stability of each complex during the simulation. D-F) Histograms of the number of HB as present during the simulation. G-I) Free energy distribution from MM/PBSA calculations. Representations in green, purple, and cyan are associated to **SAC1**, **SAC2** and **SAC3** respectively. (For interpretation of the references to colour in this figure legend, the reader is referred to the web version of this article.)

groups of the substrate **SAC3** and the (unmethylated) hydroxyl groups of DM-β-CD. These observations make sense only if the DM-β-CD macrocycle is hosting the phenyl group when forming the complex, so that the inclusion process would mostly affect the R_β and R_γ rotations (corresponding to the styryl group, Fig. 1).

For each of the SACs, DM-β-CD was found to have higher binding constants, making it a better overall host compared to β-CD (Table 1). This finding is in line with the results of the MD simulations for each dye in its ground state and with previous reports for the guests methyl orange and 8-anilino-1-naphthalenesulfonate

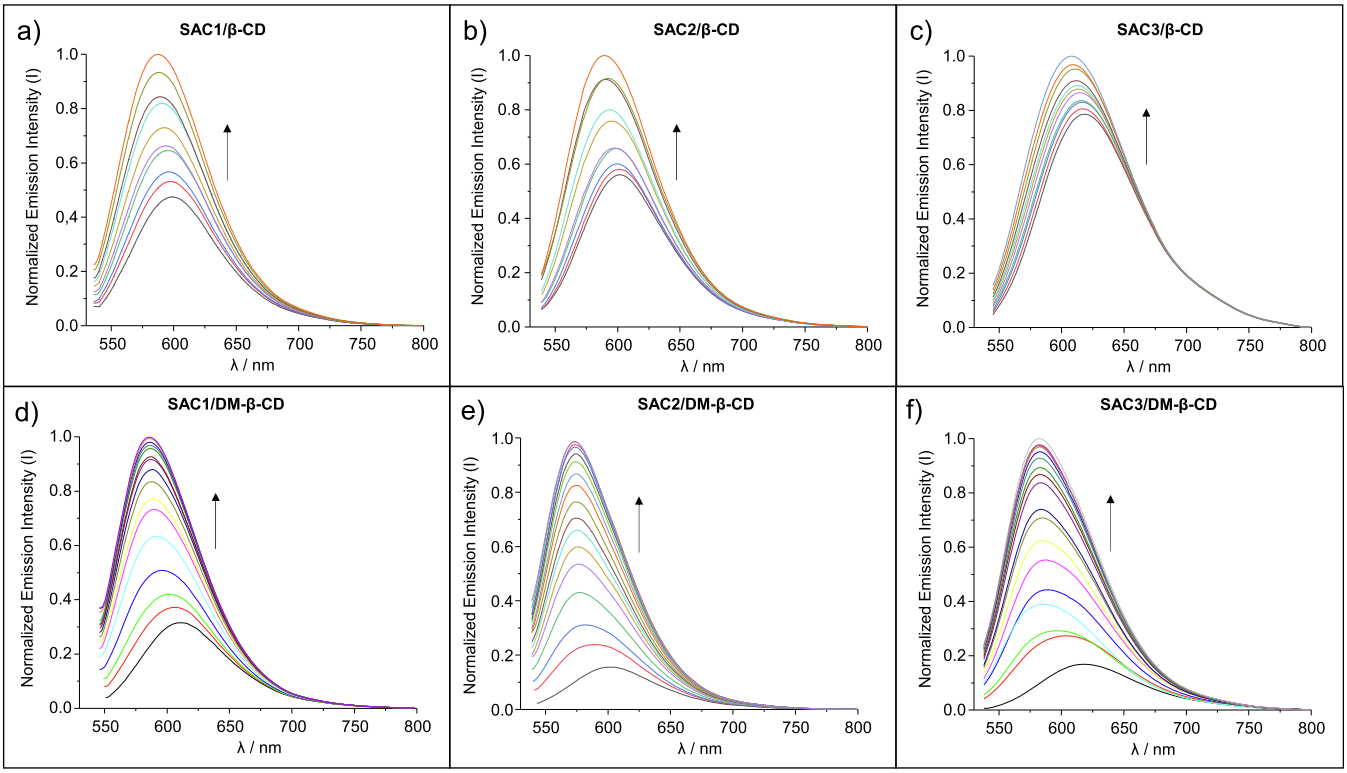

Fig. 6. Modification of the emission spectra by titrations with β-CD and DM-β-CD for the SAC compounds (1.5 μM in 30% v/v methanol and T = 25.0 °C): (a) SAC1/β-CD, (b) SAC2/β-CD, (c) SAC3/β-CD, (d) SAC1/DM-β-CD, (e) SAC2/DM-β-CD and (f) SAC3/DM-β-CD.

Table 1
Binding constants for a 1:1 model ($K_{1:1}$) between the SACs and the macrocycles: β-CD and DM-β-CD.

Macrocycle	Compound	$K_{1:1}$ (M^{-1})
β-CD	SAC1	875 ± 126
	SAC2	663 ± 70
	SAC3	537 ± 32
DM-β-CD	SAC1	8911 ± 230
	SAC2	8872 ± 368
	SAC3	20921 ± 907

[30,31]. The lower values of the binding constants for β-CD are attributed to the fact that β-CD has, for the most part, its hydroxyls focused on the formation of intramolecular hydrogen bonds, which grants it greater rigidity and diminishes its capacity to form intermolecular hydrogen bonds [32,37]. However, DM-β-CD cannot form intramolecular hydrogen bonds due to methylation in its primary face, therefore it is more flexible [37]. This flexibility could result in DM-β-CD having greater adaptability towards the substrates. A remarkable feature in DM-β-CD is that, although it does not present intramolecular hydrogen bonds, its secondary hydroxyls can form these bonds, improving its affinity with hydrogen bond accepting guests in contrast to β-CD [37]. Additionally, the hydrophobic effect is one of the phenomena that is attributed to favour DM-β-CD as a host over β-CD, as a consequence of a greater apolar depth of the cavity granted by the methyl substituents in the DM-β-CD [32].

3.3. Stokes shift (SS) and emission quantum yield (Φ_E)

Some relevant photophysical parameters such as Stokes Shift (SS) and emission Quantum Yield for **SAC1-3** dyes and their complexes with β-CD and DM-β-CD are summarized in Table 2.

As shown in Table 2, no appreciable solvatochromic absorption effect resulting from the formation of the complex is observed, since the maximum absorption wavelengths (λ_{abs}) of the substrates do not vary appreciably in the presence of β-CD and DM-β-CD. This means that the effect of both macrocycles on the Stokes shift (SS) of the dyes once the complex is formed depends only on the maximum emission wavelength in the absence and presence of the macrocycle. The maximum emission wavelength of the free substrates is around 600 nm, giving rise to SS between 3477 and 4431 cm^{-1} (see Table 2).

In the presence of macrocycles (β-CD or DM-β-CD), the Stokes Shifts of **SAC1-3** dyes are reduced, suggesting that intramolecular charge transfer (ICT) in substrates is disfavored in supramolecular inclusion. In this line, other studies have demostrated that the ICT process is inhibited in the relatively reduced polarity inside β-CD cavity [33,34]. Also it is important to consider the size of the tested cavity to regulate a particular photoprocess [34].

In fact, there are two ways in which the CD-host may be disfavoring charge transfer in the excited state of **SAC1-3** substrates: *i*) by decreasing the polarity of the environment surrounding the fluorophore as it enters the hydrophobic cavity of the host (ICT reduction), and/ or *ii)* by restricting the intramolecular R_β and/ or R_γ rotations of the substrates in the same inclusion process (TICT restriction).

On the other hand, the emission quantum yields of the substrates **SAC1-3** (Φ_E^G) increased in the presence of β-CD and DM-β-CD (Table 2), where **SAC3** was the substrate that presented the greatest increase in its Φ_E in the presence of DM-β-CD (≈6-fold). Interestingly, SAC3@DM-β-CD was the complex that presented the highest binding constant of the series (Table 1).

Furthermore, a linear relationship between the effect of the host on the emission quantum yield of the substrates $\left(\Phi_E^{HG}/\Phi_E^G\right)$ and the observed binding constant is obtained (Fig. 7A). A trend can

Table 2
Photophysical characteristics: free substrates and their complexes.[a]

Species	λ_{abs} (nm)	λ_{em} (nm)	λ_{ex} (nm)	SS (cm^{-1})	Φ_E	ΔSS (cm^{-1})	Φ_E^{HG}/Φ_E^G
SAC1	483	594	483	3869	0.144 ± 0.008	–	–
SAC2	493	595	493	3477	0.112 ± 0.008	–	–
SAC3	487	621	489	4431	0.054 ± 0.002	–	–
SAC1@β-CD	483	585	487	3610	0.249[b] ± 0.016	−259	1.73
SAC2@β-CD	493	582	493	3102	0.252[b] ± 0.016	−375	2.25
SAC3@β-CD	487	615	490	4274	0.058[b] ± 0.002	−157	1.07
SAC1@DM-β-CD	483	573	487	3252	0.500 ± 0.016	−617	3.47
SAC2@DM-β-CD	493	568	493	2678	0.409 ± 0.013	−799	3.65
SAC3@DM-β-CD	489	576	490	3089	0.332 ± 0.011	−1342	6.15

[a] MeOH (30 % v/v) at pH 2.5 and 25.0 °C.
[b] Φ_E corrected excluding the contribution of the free substrate (Supplementary material). λ_{abs}, λ_{em} and λ_{ex} are the absorbance, emission and excitation maxima of substrate (SAC), respectively.

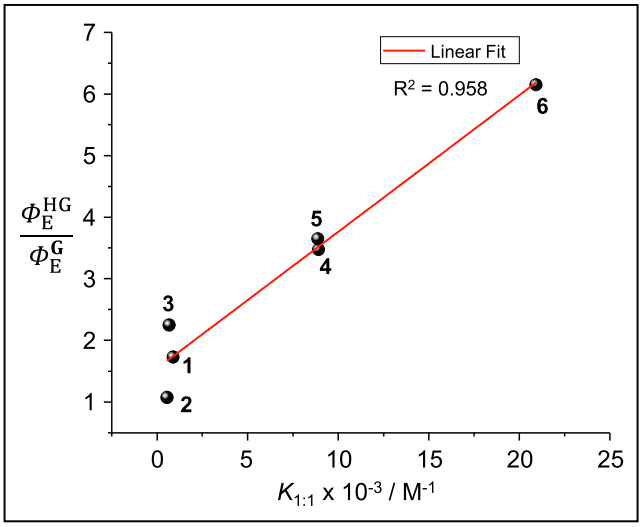

Fig. 7A. Φ_E^{HG}/Φ_E^G *versus* binding constants $K_{1:1}$ for the complexes: 1(SAC3@β-CD), 2 (SAC1@β-CD), 3(SAC2@β-CD), 4(SAC1@DM-β-CD), 5(SAC2@DM-β-CD) and 6 (SAC3@DM-β-CD).

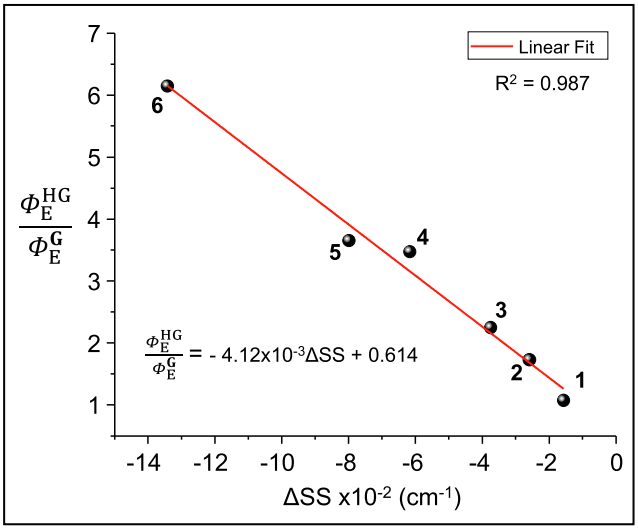

Fig. 7B. Φ_E^{HG}/Φ_E^G *versus* the change in the Stokes shift (ΔSS) for the complexes: 1 (SAC3@β-CD), 2(SAC1@β-CD), 3(SAC2@β-CD), 4(SAC1@DM-β-CD), 5(SAC2@DM-β-CD) and 6(SAC3@DM-β-CD).

be seen in which the higher the binding constant, the greater the increase in the emission quantum yield of the substrate in the complex. As the binding constant is a measure of the strength of the interaction between the host and the guest, it can be inferred that the inclusion complexes with higher binding constants heavily restrict the non-radiative paths given by the intramolecular rotations R_β and/or R_γ of the SACs, resulting in an increase in the Φ_E. These rotational restrictions induced by the macrocycles (β-CD or DM-β-CD) would also imply a disfavor of the TICT in the substrate, as above mentioned, resulting in a decrease in its SS.

Interestingly, the decrease in SS and the increase in Φ_E of **SAC1-3** substrates when forming the complex can be seen in Fig. 7B**.** This linear correlation (R^2 = 0.987) between the change in Stokes shift (ΔSS) and the change in quantum yield of **SAC1-3** upon supramolecular inclusion suggests that the rotations R_β and/or R_γ of **SAC1-3** play a significant role in the emission decay and in the Stokes shift. In other words, if the intramolecular rotations of the **SAC1-3** and the TICT are restricted, the Stokes shift decreases, disfavoring the non-radiative pathways produced by such rotations and, therefore, increasing the observed emission quantum yield.

To support these findings, computational simulations were carried out at the Density Functional Theory level (DFT). A linear correlation (R^2 = 0.983) was observed between the emission intensity and the Stokes shift in **SAC1** when the dihedral angle R_β of 180° was gradually rotated −70° and 70° (Fig. 8). This finding supports the notion of intramolecular rotations having an impact on the observed relationship between the emission decay and the Stokes shift.

On the other hand, rotations in R_γ were also evaluated (Fig. S3). However, the correlation between emission decay and ΔSS was less linear (R^2 = 0.930) than the relationship obtained when the dihedral angle R_β is rotated. In addition, the maximum ΔSS for R_γ was 7.8 times lower than that obtained in rotations of R_β. This suggests that rotations in R_γ do not exert a relevant effect on the SS of the SACs compared to rotations in R_β.

Given the computational results (Fig. 8), the linear correlation obtained between the change in the Stokes shift (ΔSS) and the change in the quantum yield of the SACs in the presence of cyclodextrins (Fig. 7B) can be explained considering that the rotational degrees of freedom of the SACs is the most important factor affected by the formation of the complex. This consideration is reasonable when taking into account that both β-CD and DM-β-CD have similar polarity. In fact, other reports have demonstrated that the internal polarity of β-CD is similar to that of ethanol [35] and the cavity of DM-β-CD have polarity similar to that of alcohol–water mixtures [36], meaning that the change in the environment surrounding the SAC dyes entering each of the cyclodextrin cavities (from DM-β-CD to β-CD) is comparable. It is important to mention, that when **SAC1** is dissolved in different organic solvents, the linear correlation between Φ_E and SS does not take place [11], possibly due to multiple factors, one of which could be intramolecular rotations.

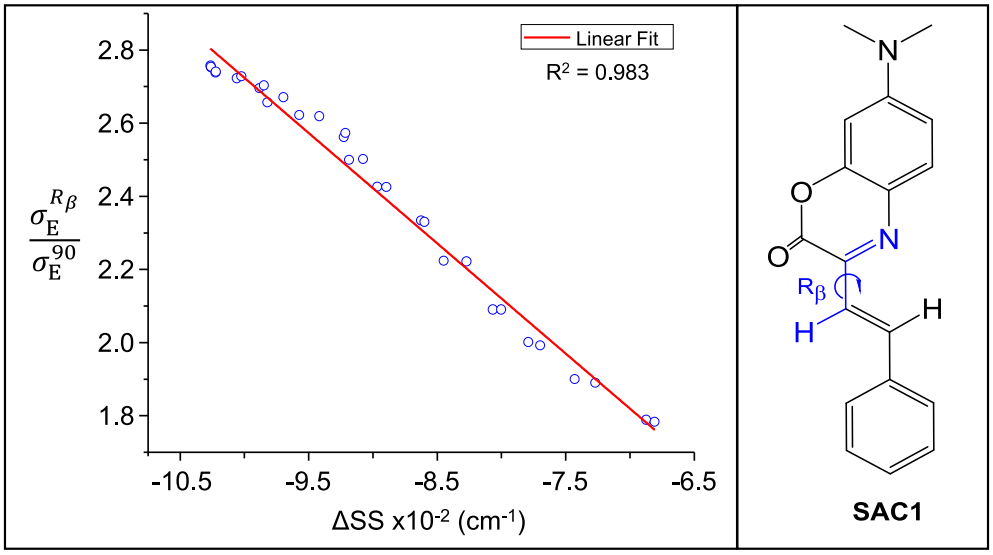

Fig. 8. Relative emission oscillator strength ($\sigma_E^{R_\beta}/\sigma_E^{90}$) *versus* variations in Stokes shifts (ΔSS). $\sigma_E^{R_\beta}$ denotes the emission oscillator strength for a specific R_β dihedral rotation. R_β = 90° was used as reference. Rotations were carried out gradually around an angle of 180° in a range of 110°–250° by ORCA software, using B97-3c as a theory level.

4. Conclusions

The fluorescence intensities of **SAC1-3** dyes were evidently enhanced by forming an equimolar inclusion complex with cyclodextrins, with higher $K_{1:1}$ values for DM-β-CD compared to β-CD. Through molecular dynamics simulation, an inclusion pattern was proposed to help explain the inclusion mode and the higher stability for DM-β-CD complexes.

The linear negative correlation between the Stokes shift and the emission quantum yield in SACs, in the presence of cyclodextrins, is a consequence of the reduced degrees of freedom of the intramolecular rotation R_β when entering the cavity of the macrocycle. The greater restriction on R_β is due to: *i*) a stronger π-conjugation, allowing for a less polarized excited state and therefore a smaller Stokes shift; *ii*) reduction of non-radiative paths product of intramolecular rotations, therefore, higher emission quantum yield. In other words, the intramolecular rotation restrictions on R_β give rise to an inverse relationship between their Stokes shift and quantum yield, whereby smaller Stokes shifts correspond to greater quantum yields, and vice versa. Findings of the present study suggest that fine-tuning molecular rotation can serve as an effective strategy for optimizing the design of fluorescent organic dyes with potential applications in diverse areas, including biosensors, organic light-emitting diodes OLEDs, photosensitizers, and fluorescence imaging. Further research is needed to explore the mechanisms underlying the observed effects and to expand the range of fluorescent materials that can benefit from this approach.

CRediT authorship contribution statement

Jackson J. Alcázar: Conceptualization, Investigation, Formal analysis, Writing, review and editing. **Luis García-Río:** Conceptualization, Investigation, Formal analysis, Writing, review and editing, Supervision, Validation original draft. **Agustín I. Robles:** Conceptualization, Investigation, Formal analysis. **Luis Dinamarca-Villarroel:** Conceptualization, Investigation, Formal analysis. **Angélica Fierro:** Conceptualization, Investigation, Formal analysis. **José G. Santos:** Writing, review and editing, Supervision, Validation original draft. **Margarita E. Aliaga:** Writing, review and editing, Supervision, Validation original draft, Funding acquisition and Project administration.

Data availability

The authors are unable or have chosen not to specify which data has been used.

Declaration of Competing Interest

The authors declare that they have no known competing financial interests or personal relationships that could have appeared to influence the work reported in this paper.

Acknowledgements

This work was supported by FONDECYT grants N° 1210751 and 1221030, Fondequip EQM170172. J.J.A. is grateful for the CONICYT Doctoral Fellowship 21170793.

Powered@NLHPC: This research was partially supported by the supercomputing infrastructure of the NLHPC (ECM-02). The authors wish to thank Alessandra Misad for proofreading the manuscript.

Appendix A. Supplementary material

Supplementary data to this article can be found online at https://doi.org/10.1016/j.molliq.2023.121790.

References

[1] M.M.L. Kadam, D.S. Patil, N. Sekar, Red emitting coumarin based 4, 6-disubstituted-3-cyano-2-pyridones dyes – synthesis, solvatochromism, linear and non-linear optical properties, J. Mol. Liq. 276 (2019) 385–398, https://doi.org/10.1016/j.molliq.2018.11.164.

[2] L. Stroea, M. Murariu, V. Melinte, Fluorescence quenching study of new coumarin-derived fluorescent imidazole-based chemosensor, J. Mol. Liq. 318 (2020), https://doi.org/10.1016/j.molliq.2020.114316.

[3] N. Zhao, Y. Li, W. Yin, J. Zhuang, Q. Jia, Z. Wang, N. Li, Controllable Coumarin-based NIR fluorophores: selective subcellular imaging, cell membrane potential indication, and enhanced photodynamic therapy, ACS Appl. Mater. Interfaces. 12 (2020) 2076–2086, https://doi.org/10.1021/acsami.9b18666.

[4] M.V. Sednev, V.N. Belov, S.W. Hell, Fluorescent dyes with large Stokes shifts for super-resolution optical microscopy of biological objects: a review, Methods Appl. Fluoresc. 3 (2015), https://doi.org/10.1088/2050-6120/3/4/042004.

[5] C. Trebaul, J. Roncali, F. Garnier, R. Guglielmetti, Synthesis and fluorescence analysis of 3-substituted 7-dialkylamino-2H-l,4-benzoxazin-2-ones, Bull. Chem. Soc. Jpn. 60 (1987) 2657–2662, https://doi.org/10.1246/bcsj.60.2657.

[6] Q. Chen, W. Liu, Y. Han, L. Li, F. Yuan, L. Long, K. Wang, Accurately monitoring of sulfur dioxide derivatives in agricultural crop leaf tissues by a novel sensing system, Sensors Actuators, B Chem. 323 (2020), https://doi.org/10.1016/j.snb.2020.128711.
[7] Y. Lu, H. Li, Q. Yao, W. Sun, J. Fan, J. Du, J. Wang, X. Peng, Lysozyme-targeted ratiometric fluorescent probe for SO2 in living cells, Dye. Pigment. 180 (2020), https://doi.org/10.1016/j.dyepig.2020.108440.
[8] H. Agarwalla, H.A. Anila, F. Ali, S.R. Pradhan, B. Ganguly, S.K. Pramanik, A. Das, Fluorescent chemodosimeter for quantification of cystathionine-γ-synthase activity in plant extracts and imaging of endogenous biothiols, Chem. Commun. 54 (2018) 9079–9082, https://doi.org/10.1039/c8cc04296a.
[9] M. Yu, W. Du, H. Li, H. Zhang, Z. Li, Near-infrared ratiometric fluorescent detection of arginine in lysosome with a new hemicyanine derivative, Biosens. Bioelectron. 92 (2017) 385–389, https://doi.org/10.1016/j.bios.2016.10.090.
[10] J. Fan, W. Sun, M. Hu, J. Cao, G. Cheng, H. Dong, K. Song, Y. Liu, S. Sun, X. Peng, An ICT-based ratiometric probe for hydrazine and its application in live cells, Chem. Commun. 48 (2012) 8117–8119, https://doi.org/10.1039/c2cc34168a.
[11] S. Fery-Forgues, M.T. Le Bris, J.C. Mialocq, J. Pouget, W. Rettig, B. Valeur, Photophysical properties of styryl derivatives of aminobenzoxazinones, J. Phys. Chem. 96 (1992) 701–710, https://doi.org/10.1021/j100181a035.
[12] F. Vollmer, W. Rettig, E. Birckner, Photochemical mechanisms producing large fluorescence stokes shifts, J. Fluoresc. 4 (1994) 65–69, https://doi.org/10.1007/BF01876657.
[13] J.J. Alcázar, E. Márquez, L. García-Río, A. Robles-Muñoz, A. Fierro, J.G. Santos, M. E. Aliaga, Changes in protonation sites of 3-styryl derivatives of 7-(dialkylamino)-aza-coumarin dyes induced by cucurbit[7]uril, Front. Chem. 10 (2022) 273, https://doi.org/10.3389/fchem.2022.870137.
[14] R.N. Dsouza, U. Pischel, W.M. Nau, Fluorescent dyes and their supramolecular host/guest complexes with macrocycles in aqueous solution, Chem. Rev. 111 (2011) 7941–7980, https://doi.org/10.1021/cr200213s.
[15] G. Jones, W.R. Jackson, A.M. Halpern, Medium effects on fluorescence quantum yields and lifetimes for coumarin laser dyes, Chem. Phys. Lett. 72 (1980) 391–395, https://doi.org/10.1016/0009-2614(80)80314-9.
[16] G. Jones, W.R. Jackson, S. Kanoktanaporn, A.M. Halpern, Solvent effects on photophysical parameters for coumarin laser dyes, Opt. Commun. 33 (1980) 315–320, https://doi.org/10.1016/0030-4018(80)90252-7.
[17] G. Jones, W.R. Jackson, C.Y. Choi, W.R. Bergmark, Solvent effects on emission yield and lifetime for coumarin laser dyes. Requirements for a rotatory decay mechanism, J. Phys. Chem. 89 (1985) 294–300, https://doi.org/10.1021/j100248a024.
[18] B.G. Poulson, Q.A. Alsulami, A. Sharfalddin, E.F. El Agammy, F. Mouffouk, A.-H. Emwas, L. Jaremko, M. Jaremko, Cyclodextrins: structural,chemical, and physical properties, and applications, Polysaccharides 3 (2021) 1–31, https://doi.org/10.3390/polysaccharides3010001.
[19] P. Thordarson, Determining association constants from titration experiments in supramolecular chemistry, Chem. Soc. Rev. 40 (2011) 1305–1323, https://doi.org/10.1039/c0cs00062k.
[20] A.M. Brouwer, Standards for photoluminescence quantum yield measurements in solution (IUPAC technical report), Pure Appl. Chem. 83 (2011) 2213–2228, https://doi.org/10.1351/PAC-REP-10-09-31.
[21] G.A. Crosby, Measurement of photoluminescence quantum yields, Chem. Int. 37 (2015) 991–1024, https://doi.org/10.1515/ci-2015-0521.
[22] M. Iglesias, B. Orge, J. Tojo, Refractive indices, densities and excess properties on mixing of the systems acetone + methanol + water and acetone + methanol + 1-butanol at 298.15 K, Fluid Phase Equilib. 126 (1996) 203–223, https://doi.org/10.1016/S0378-3812(96)03130-5.
[23] M. Adachi, B. Mikami, T. Katsube, S. Utsumi, Crystal structure of recombinant soybean β-amylase complexed with β-cyclodextrin, J. Biol. Chem. 273 (1998) 19859–19865, https://doi.org/10.1074/jbc.273.31.19859.
[24] T. Petrenko, O. Krylova, F. Neese, M. Sokolowski, Optical absorption and emission properties of rubrene: Insight from a combined experimental and theoretical study, New J. Phys. 11 (2009), https://doi.org/10.1088/1367-2630/11/1/015001.
[25] J.G. Brandenburg, C. Bannwarth, A. Hansen, S. Grimme, B97–3c: A revised low-cost variant of the B97-D density functional method, J. Chem. Phys. 148 (2018), https://doi.org/10.1063/1.5012601.
[26] F. Neese, F. Wennmohs, U. Becker, C. Riplinger, The ORCA quantum chemistry program package, J. Chem. Phys. 152 (2020), https://doi.org/10.1063/5.0004608.
[27] E.E. Tucker, S.D. Christian, Vapor pressure studies of benzene-cyclodextrin inclusion complexes in aqueous solution, J. Am. Chem. Soc. 106 (1984) 1942–1945, https://doi.org/10.1021/ja00319a007.
[28] G.L. Bertrand, J.R. Faulkner, S.M. Han, D.W. Armstrong, Substituent effects on the binding of phenols to cyclodextrins in aqueous solution, J. Phys. Chem. 93 (1989) 6863–6867, https://doi.org/10.1021/j100355a057.
[29] H. Kim, H.W. Kim, S. Jung, Aqueous solubility enhancement of some flavones by complexation with cyclodextrins, Bull. Korean Chem. Soc. 29 (2008) 590–594, https://doi.org/10.5012/bkcs.2008.29.3.590.
[30] A. Pereira-Vilar, M. Martin-Pastor, M. Pessêgo, L. García-Río, Supramolecular recognition induces nonsynchronous change of dye fluorescence properties, J. Org. Chem. 81 (2016) 6587–6595, https://doi.org/10.1021/acs.joc.6b01230.
[31] R.I. Gelb, L.M. Schwartz, Complexation of adamantane-ammonium substrates by beta-cyclodextrin and its O-methylated derivatives, J. Incl. Phenom. Mol. Recognit. Chem. 7 (1989) 537–543, https://doi.org/10.1007/BF01080464.
[32] G. Wenz, Influence of intramolecular hydrogen bonds on the binding potential of methylated β-cyclodextrin derivatives, Beilstein J. Org. Chem. 8 (2012) 1890–1895, https://doi.org/10.3762/bjoc.8.218.
[33] D.W. Cho, Y.H. Kim, S.G. Kang, M. Yoon, D. Kim, Cyclodextrin effects on intramolecular charge transfer of 2-biphenylcarboxylic acid: a pre-twisted molecule, J. Chem. Soc. - Faraday Trans. 92 (1996) 29–33, https://doi.org/10.1039/ft9969200029.
[34] A. Mallick, P. Purkayastha, N. Chattopadhyay, Photoprocesses of excited molecules in confined liquid environments: an overview, J. Photochem. Photobiol. C Photochem. Rev. 8 (2007) 109–127, https://doi.org/10.1016/j.jphotochemrev.2007.06.001.
[35] A. Heredia, G. Requena, F.G. Sánchez, An approach for the estimation of the polarity of the β-cyclodextrin internal cavity, J. Chem. Soc. Chem. Commun. (1985) 1814–1815, https://doi.org/10.1039/C39850001814.
[36] L. García-Río, R.W. Hall, J.C. Mejuto, P. Rodriguez-Dafonte, The solvolysis of benzoyl halides as a chemical probe determining the polarity of the cavity of dimethyl-β-cyclodextrin, Tetrahedron 63 (2007) 2208–2214, https://doi.org/10.1016/j.tet.2006.12.083.
[37] N. Geue, J.J. Alcázar, P.R. Campodónico, Influence of β-Cyclodextrin Methylation on Host-Guest Complex Stability: A Theoretical Study of Intra- and Intermolecular Interactions as Well as Host Dimer Formation, Molecules 28 (2023) 2625, https://doi.org/10.3390/molecules28062625.